Saudi Journal of Biological Sciences 27 (2020) 1155–1162

Contents lists available at ScienceDirect

Saudi Journal of Biological Sciences

journal homepage: www.sciencedirect.com

Original article

Cancer inhibition mechanism of lung cancer mouse model based on dye trace method

Wei Zhang [a,1], Hongyan Shu [b,1], Lixin Fang [a], Ning Tang [a], Yucai Li [a], Bingrong Guo [a], Fanhui Meng [b,*]

[a] Department of Thoracic Surgery, Linzi District People's Hospital, Zibo City 255400, China
[b] Department of Endocrinology, Linzi District People's Hospital, Zibo City 255400, China

ARTICLE INFO

Article history:
Received 14 October 2019
Revised 23 December 2019
Accepted 25 December 2019
Available online 3 January 2020

Keywords:
Lung cancer
Mouse model
Dye tracer method
Cancer inhibition mechanism

ABSTRACT

To minimize the incidence and mortality of cancer, dye trace method was used to explore the mechanism of drug inhibition. 60 mice were selected as the research objects and randomly divided into five groups: model group, shikonin group, aconitine group, notoginsenoside R1 group, and compound group. When establishing the model, begin to administrate the medicine by gavage. The permeability of lung barrier was measured, and H.E staining, immunohistochemical staining, and Western blot test were carried out. The results showed that the mice in model group had decreased autonomic activity, increased permeability of the lung barrier, white nodules on the lung tissue, decreased protein expression related to cell proliferation and differentiation, and decreased protein expression associated with cell proliferation and differentiation, increased expression of related proteins in cancer stem cells, and low level of cell-linked communication. And the incidence of lung cancer in the model group mice was 100%. The histopathological changes in mice were improved to varying degrees after the intervention of the three drugs. Especially in the compound group, the incidence of lung cancer decreased to 8.3%. This study demonstrated that the combination of shikonin, aconitine and notoginsenoside R1 had a good anti-cancer effect, which provided a theoretical basis for clinical research.

1. Introduction

Nowadays, cancer has become a common disease that seriously endangers human life and health. The incidence and mortality of lung cancer are quite high worldwide, and it is an uncontrollable malignant tumor (Zhang et al., 2018). In China, the incidence and mortality of lung cancer in male are the first in cancer, and the incidence and mortality of lung cancer in female are in the second and first respectively (Szczepny et al., 2017). Therefore, the treatment of lung cancer is a hot issue that people and medical researchers continue to pay attention to (Yan et al., 2017). At present, the main methods for treating cancer are surgical resection, radiotherapy and chemotherapy, but nearly half of the patients are unable to receive treatment for various reasons, so finding an alternative therapy that can effectively treat cancer has become a top priority (Luo et al., 2018; Ramirezalcantara et al., 2017). The process of cancer production and development is a disease with complex pathogenesis, complex disease course and interaction of various conditions. It generally undergoes three stages, namely the primary stage, the cancer-promoting stage and the evolutionary stage (Meraz et al., 2017; Ehlerding et al., 2017). The primary stage of cancer is an irreversible mutation process. Cancer cells are not active at the initial stage. As the carcinogens participate in the circulation, the tumor cells increase, DNA is damaged and adduct was formed, the duration of this process is not too long (Harshbarger et al., 2017; Sato et al., 2017). If anti-cancer drugs can block or inhibit the circulating metabolism of carcinogen and growth of tumor cell, it may achieve the goal of preventing cancer (Pyo et al., 2017). A large number of studies have found that the tumor microenvironment provides a good living environment for tumor cells, and this microenvironment plays a key role in the progression of many tumor-related diseases such as tumor enlargement, tumor invasion, and tumor metastasis (Lakshmanan et al., 2017). Chronic inflammatory microenvironment can affect the normal

* Corresponding author at: Department of Thoracic Surgery, Linzi District People's Hospital, No. 139 Huangong Road, Zibo City 255400, China.
E-mail address: drmengfanhui2012@126.com (F. Meng).
[1] These author contributed equally to this work.

Peer review under responsibility of King Saud University.

Production and hosting by Elsevier

https://doi.org/10.1016/j.sjbs.2019.12.040
1319-562X/

surrounding environment of cells, accumulating inflammatory cells and causing oxidative damage to normal cells. Mutated cells can grow without constraint in this microenvironment, ultimately leading to cancer (Perepelyuk et al., 2017).

Tumor development and wound repair are the result of interaction of a variety of genetic factors. The nature of the cells themselves, the microenvironment in which they are located, and the intersection of the signaling pathways are all factors that affect them. The destruction of wounds by physical, chemical or biological factors can lead to the development of cancer (Menter et al., 2017; Best et al., 2018). The basic goal of cancer prevention is to reduce morbidity and mortality. To reduce the mortality rate of cancer requires finding effective means to treat cancer, and reducing the incidence of cancer requires finding effective preventive measures. Effective prevention of cancer is the best way to stop cancer, and Chinese medicine has shown great advantages in preventing disease (Li et al., 2019). The pathogenesis and disease progression of urethane-induced lung cancer in mice is very similar to that in human lung cancer. Using this model to study drug prevention, on the one hand, can enhance the understanding of the pathogenesis of cancer, on the other hand, it provides a basis for research and prevention of cancer.

At present, although there are many studies on the mechanism of cancer, there are few from the perspective of wound healing microenvironment. The innovation of this paper is to put forward the scientific hypothesis that "wound healing microenvironment prevents the occurrence of cancer", and to explore the wound healing effect of aconitine, shikonin, and notoginsenoside R1. Studying the improvement of tumor microenvironment by Chinese medicine has avery important relationship with the development and progression of cancer. Hence, to reduce the incidence and mortality of cancer, in this study, urethane-induced mouse lung cancer model was used to observe the prevention and treatment effect of aconitine, shikonin and notoginsenoside R1 in lung cancer, and to study whether these three traditional Chinese medicines can alleviate or prevent the carcinogenic process in mice; and based on this, to explore new ways to prevent and treat cancer.

2. Materials and methods

2.1. Animals

60 C57BL/6 mice, female, weighing between 16 g and 21 g, around 8 weeks old were purchased from Hunan Slake Jingda Laboratory Animal Co., Ltd., China. The feeding temperature was constant at 20–26 °C, and the mice were given free access to move, eat and drink. The mice were divided into 5 groups according to the random principle, with 12 in each group, the 1st group was model group, the 2nd group was shikonin group, the 3rd group was aconitine group, the 4th group was notoginsenoside R1 group, and the 5th group was compound group.

2.2. Construction of lung cancer mouse model

Modeling: All mice were injected intraperitoneally with a solution of urethane (China National Chemical Reagent Corporation, Ltd.) configurated by double distilled water (600 mg/kg), once a week for 10 weeks.

Administration: administration of intragastric administration was started on the day of modeling. The drugs were all dissolved with 0.5% CMC-Na. The shikonin group was given a dose of 2 mg/kg of shikonin (Sigma-Aldrich Company, USA), and the aconitine group was given a dose of 0.2 mg/kg of aconitine (Sigma-Aldrich Company, USA), and the notoginsenoside R1 group was administered with a dose of 20 mg/kg of notoginsenoside R1 (Sigma-Aldrich Company, USA), and the compound group was given a dose of compound of the three: 2 mg/kg of shikonin, 0.2 mg/kg of aconitine and 20 mg/kg. The control group was given an equal dose of 0.5% CMC-Na. Once a day for 20 weeks. The autonomic activity and mortality of the mice were continuously recorded weekly. The score of mouse's autonomic activity was measured by YLS-1A multifunctional mouse autonomic activity recorder (Anhui Huaibei Zhenghua biological Instrument Co., Ltd., China). The higher the score was, the more autonomic activity the mouse had.

2.3. Lung barrier permeability test

4 mice were selected from each group. The tail vein of the mouse was injected with 2% Evans Blue (Bio-Rad Company, USA) at a dose of 2 mL/kg. After waiting for 30 min for the mice to be successfully anesthetized, the mouse chest was opened, the sterile saline was perfused from the heart, the right atrium was cut, and the blood in the pulmonary blood vessels of the mice was rinsed. Absorb excess water with filter paper and accurately weigh the lung tissue. After weighing, the lung tissue was cut, and the normal saline was added in a ratio of lung weight (g) to normal saline at 1:9, and the lung tissue was ground to obtain a homogenate, and formamide was added at a dose of 2 mL/100 mg (lung tissue) and mixed with lung tissue. The mixture was homogenized and incubated in a 37° C incubator for 24 h. The homogenate was centrifuged and the supernatant was discarded. The distilled water was used as a blank control group, and the absorbance was measured at 620 nm. The lung barrier permeability was reflected by the standard curve in terms of the amount of dye extracted per unit tissue.

2.4. H. E staining test

4 mice were selected from each group. After the mice blood was collected from the eyeballs, the lungs of the mice were immediately taken, washed three times with PBS solution, fixed in 4% formaldehyde for 48 h to dehydrate, and the tissue was cut and put into the embedding box, rinsed with running water overnight to remove the fixative. After that, the tissue was dehydrated with 70% ethanol, 80% ethanol and 90% ethanol for 1 h, and dehydrated with 95% ethanol and absolute ethanol for 2 h. After soaking in xylene for 1 h, the tissue was transparent and then dipped in wax. After dipping the wax, the sample was taken out, and the bottom of the metal box for embedding was poured into a layer of wax at first. After the wax was slightly solidified, the mouse lung tissue was placed into the metal embedding box, and paraffin was added on the ice box and stored in the refrigerator. When it is necessary to use, the embedded tissue was taken out, and the wax block was cut into 6 μm sections, placed in hot water at 45 °C to stretch it., and picked up with a glass slide prepared in advance to perform baking. After the slices were dried for 2 h, HE staining was performed, and the sections were placed in xylene for dewaxing. The ethanol was used to elute paraffin and xylene. Distilled water was rehydrated, and hematoxylin (Sigma-Aldrich Company, USA) was used for dyeing. Differentiated by hydrochloric acid alcohol for about 20 s, rinsed with running water overnight. The posterior section was then immersed in the eosin solution. After the staining, the section was placed in 95% ethanol to continue dehydration of the tissue, followed by dehydration in absolute ethanol, repeated twice, and then the section was made transparent with xylene, and finally sealed with a neutral gum and dried for use of the test.

2.5. Immunohistochemical coloration detection

The paraffin sections were baked at 60 °C for 1 h, dewaxed with xylene and gradient ethanol, washed with distilled water for 5 min,

rinsed with PBS for 5 min, and inactivated with endogenous peroxidase, then incubated in 3% H_2O_2 for 10 min at room temperature. Place the sections in boiling 0.01 M citrate buffer, continue to heat and boil for 5 min, stop heating and cool for 8 min, then heat and boil for another 5 min, re-cool for 10 min, use PBS to rinse 2 times for 2 min each time. Perform antigen thermal remediation and seal it. Primary antibody incubation: diluted ki67 and Cleaved Caspase-3 rabbit anti-mouse polyclonal antibody (1:50) were evenly covered on the surface of lung tissue sections and incubated at 4 °C overnight, washed with PBS for 3 times with 5 min each time and the interval of 4 min, the section can't be dry. Secondary antibody incubation: Biotinylated goat anti-rabbit IgG (1:100) was uniformly covered on a surface of a lung tissue section and incubated at 37 °C for 20 min, washed with PBS for 3 times with 5 min each time. Then the tissue was incubated with SABC reagent in a water bath for 20 min at 37 °C, and washed with PBS for 4 times with 5 min each time. After that, the section was covered with DAB for 10 min, then rinsed with running water, which play the role of anti-blue, then rinsed with running water, counterstain was carried out with hematoxylin for 30 s, rinsed with running water, quickly rinsed after color separation with 1% hydrochloric acid alcohol, and dehydrated with gradient alcohol. Finally, it was immersed in xylene for 5 min and then sealed with a neutral gum. After the cover was air-dried, it was observed under a microscope and photographed. The results were expressed by semi-quantitative method, and the staining intensity scores of the sections were scored as 0 for negative staining, 1 for weak positive staining, 2 for positive staining, and 3 for strong positive staining.

2.6. Western blot detection of protein expression in lung tissue

4 mice in each group were selected for testing. The blood in the lung tissue of the mice was washed with normal saline. Each group was weighed 1.5 g of tissue, maintained in a low temperature environment and fully ground. Each group of tissues was ground for 40 times in the same direction with the same strength. The RPPA cell lysate containing PMSF was diluted in a volume of 1:9 to prepare a lung tissue homogenate, which was lysed on ice for 30–60 min. The homogenate was shaken frequently during the lysis. After the completion of the lysis, it was accurately weighed on a balance, and centrifuged at 12,000 rpm for 10 min at 4 °C in a pre-cooled high-speed centrifuge. The supernatant was taken and dispensed into a 0.5 mL EP tube, and the remaining portion was stored at −20 °C.

A standard curve was drawn according to the specifications of the BCA Protein Quantification Kit, and then a number of 1.5 mL EP tubes were taken and 800 μL of sterile water were added into the tubes. Then, 200 μL of Coomassie Brilliant Blue was added for coloration under low temperature conditions, and 200 μL was dropped into each well, and its absorbance was measured with a microplate reader. Finally, the protein content was calculated based on the obtained standard curve. According to the measured sample protein content of each group, the loading quantity of sample was 30 μg. After the protein volume was obtained, the sample was pipetted and added to the labeled 1.5 mL EP tube, and then 5xloading buffer of same volume was added, and then made up with sterile water, mixed and boiled for 5 min, protein denaturation was promoted by high temperature.

After the concentrated gel and the separating gel are disposed, electrophoresis and membrane transfer were performed. After the membrane was transferred, the NC membrane was taken, the gel was discarded, and 2.5 g of skim milk powder was dissolved in 50 mL of PBST to prepare a 5% blocking solution, and the NC membrane was blocked for 1 h. Incubation of the primary antibody: the blocking solution was discarded, the antibody was diluted, and the band after completion of the blocking was immersed in the diluted solution, and shaken at 4 °C for 12 h under a shaker. After rewarming for 2 h, the primary antibody was discarded, washed with PBST, and washed 3 times for 5 min each time. Incubation of the secondary antibody: the secondary antibody was mixed with a 5% skim milk powder solution at a ratio of 1:2000, and after mixing, the NC membrane was incubated at room temperature for 2 h. After the incubation of the secondary antibody, the NC membrane was discarded and the secondary antibody was washed three times with PBST for 15 min each time. The NC membrane was incubated with the luminescent reaction solution for 2 min, and the protein surface of the membrane was face up to expose and develop image.

2.7. Dye tracer detection of cell gap junction communication

MLE-12 cells in logarithmic growth phase were selected, digested with 0.25% trypsin, and stopped when the cells were detached from the wall of the culture vessel. The cell concentration was calculated and the number of cells was diluted to 2×10^5/mL, 2 mL of cells were inoculated per well on the well plate. After that, the plate was incubated in a cell incubator with 5% CO^2 at 37 °C and the drug was added as it grows to saturation. The final concentration of the drug was 10 μM of urethane, 0.2 μM of shikonin, 0.02 μM of aconitine, 2 μM of notoginsenoside R1 and the combination of three drugs, 3 replicate wells were set for each well, continued to culture for 48 h. The PBS was heated to 37 °C, the cells were washed three times in succession, and the pre-warmed 0.05% fluorescent yellow PBS dye was added, 2 mL per well. A scalpel with thin blade was used to pierce the cell layer and lightly scratch it. After 3 min, the fluorescent yellow dye was discarded. The cells were washed twice with PBS, and the number of fluorescence transfer layers between the cells was observed under a microscope. There were two scratches in the cell layer of each well., 10 wells were observed and recorded according to the random principle. The number of cell layers passed from the scratch side to the adjacent cells was scored according to the fluorescence: 0 point for the cells where fluorescence was limited to the single layer of cells adjacent to the scratch; 1 point for the cells where the fluorescence was transmitted from the cell to the side of the adjacent 1–2 layers of scratch; 2 point for the cells where the fluorescence was transmitted from the cell to the side of the adjacent 2–3 layers of scratch; 3 point for the cells where the fluorescence was transmitted from the cell to the side of the adjacent 4 layers or more of scratch.

2.8. Statistical analysis

The data were obtained by SPSS17.0 software package. The experimental data were expressed as (x ± s). The difference between groups was analyzed by one-way analysis of variance. $P < 0.05$ indicated significant difference, $P < 0.01$ indicated that there was a very significant difference. The results of electrophoresis experiments were analyzed by Quantity one software. The optical density values of the bands were quantified. All the data were repeated three times, and the average value was obtained. The results were expressed as (x ± s), and the differences between the groups were statistically analyzed by T test.

3. Results and discussion

3.1. Changes in basic signs of mice

In the initial stage of intragastric administration of mice with urethane, the body weight of each group of mice decreased, and at 6–8 weeks, the body weight of the mice showed a state of initial

recovery, in which the body weight of the mice in the compound group decreased less in the descending phase. At the end of the period of urethane intragastric administration in the mice, the body weight of mice gradually recovered and showed an increasing trend. At 18 weeks, the body weight of the model group showed a slow decrease, and accompanied by a decrease in the state of the mice, while the mice in the other groups were better than the model group, and the mice in the compound group had the best state, as shown in Fig. 1.

There was a decline in the autonomic activity of mice during the initial phase of urethane administration to mice. At the end of the period of urethane intragastric administration in the mice, the autonomous activities of the mice in each group were kept at a low value. After 16 weeks, the autonomous activity of the mice in the model group was significantly reduced, and the living condition of the mice was significantly deteriorated, accompanied by a decrease in the amount of food intake and the amount of drinking water. Furthermore, the hair of mice became rough and tousled. The spontaneous activity of the mice in each group with administration of drugs did not decrease significantly and remained stable, as shown in Fig. 2.

3.2. Effects of three drugs on the incidence of lung cancer and HE staining results

The incidence of lung cancer in each group of mice is shown in Fig. 3A. The incidence of lung cancer in the model group was 100%. The incidence of lung cancer in the shikonin group, the aconitine group and the notoginsenoside R1 group decreased. There was a significant decrease in the incidence of lung cancer in the compound group. The incidence of lung cancer in the shikonin group was 75%, the incidence of lung cancer in the aconitine group was 50%, and the incidence of lung cancer in the ginsenoside R1 group was 66.7%. While the incidence of lung cancer in the compound group was only 8.3%. There was a significant increase in lung barrier permeability in the urethane-induced mouse lung cancer model. The shikonin group, the aconitine group and the notoginsenoside R1 group and the compound group all have a deduction effect on the permeability of the lung barrier, especially in the compound group, the permeability of the lung barrier has been reduced to a state close to the normal level, as shown in Fig. 3B.

After 22 weeks of experimentation, the mice were dissected and the lung tissue was taken out, and the lung illustrative diagram and H.E staining map are shown in Fig. 4. It was observed that there were obvious white nodules on the lung tissue of the mice, and the texture was hard, which was not the same as the ordinary abscess. After performing HE staining on lung tissue sections, it was observed that the lung tissue cells of the model group had nuclear aberrations, and the nucleoli became more numerous and the volume became larger, the nuclear staining was too deep, and the apoptosis is serious, the leukocyte infiltration was obvious, the chromatin was granular, and canceration appeared. The white nodules in the HE stained sections of the lung tissue of the shikonin-administered group, the aconitine-administered group and the notoginsenoside R1-administered group were denser. And there was no large cavity, the nucleus was small, and the inside of the gland was only infiltrated by a small amount of tumor cells. The pathological changes of lung tissue in the compound drug group were basically the same as those in normal mice.

3.3. Immunohistochemistry results

As shown in Fig. 5, the positive phenomenon appeared after section staining. By semi-quantitative analysis and scoring of

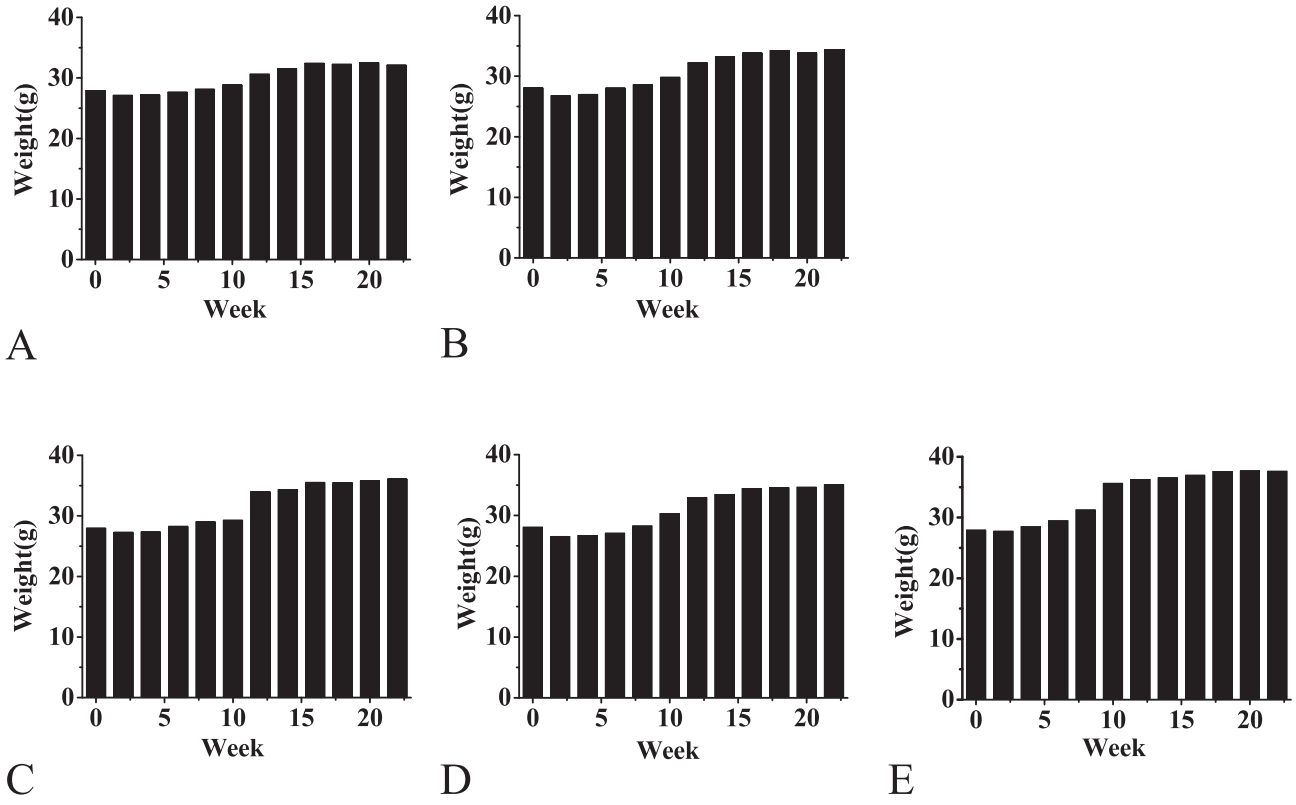

Fig. 1. Weight recording of different groups of mice during the experiment. (A: Body weight of model group during the experiment B: Body weight of shikonin group during the experiment C: Body weight of aconitine group during the experiment D: Body weight of notoginsenoside R1 group during the experiment E: Body weight of compound group during the experiment).

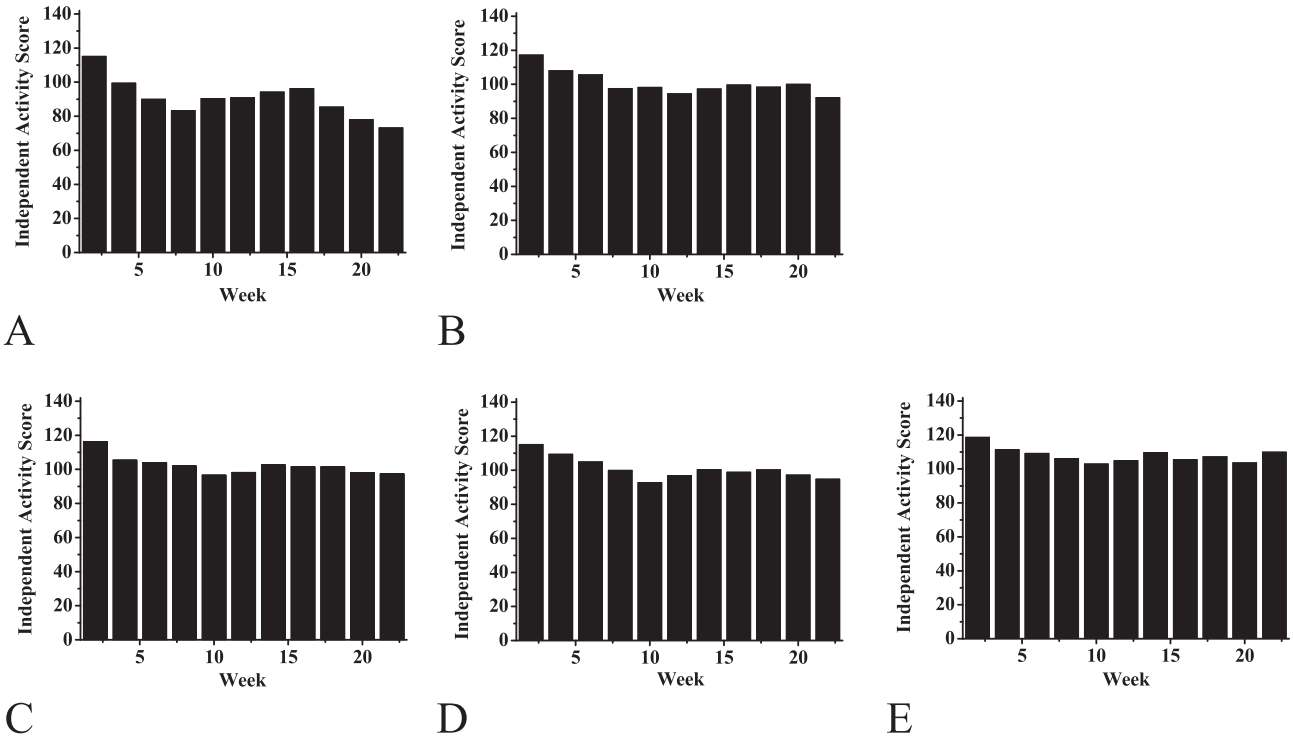

Fig. 2. Autonomous activity scores of different groups of mice during the experiment. (A: Autonomous activity score of model group during the experiment B: Autonomous activity score of shikonin group during the experiment C: Autonomous activity score of aconitine group during the experiment D: Autonomous activity score of notoginsenoside R1 group during the experiment E: Autonomous activity score of compound group during the experiment).

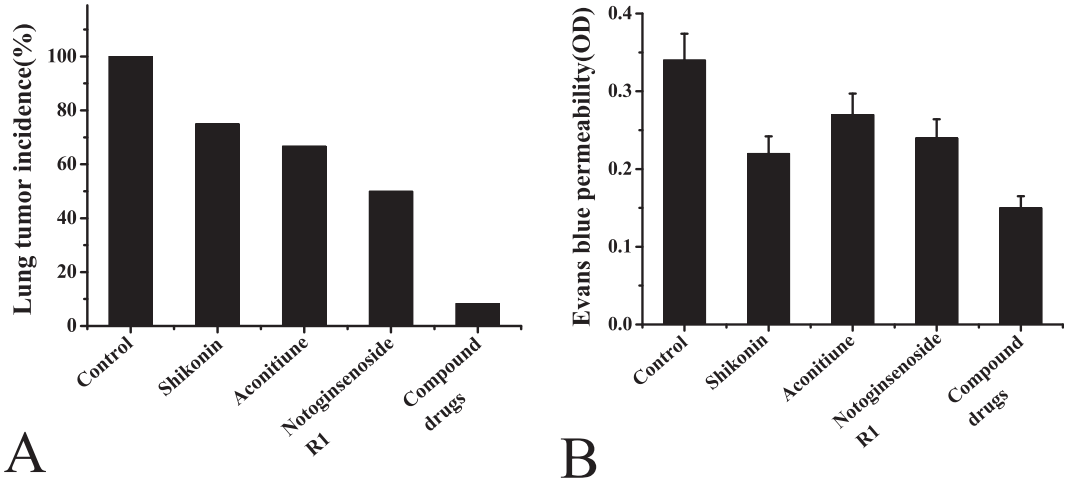

Fig. 3. Effects of different drugs on urethane-induced lung cancer. (A: effects of different drugs on the incidence of lung cancer in mice B: effects of different drugs on lung barrier permeability of mouse lung cancer).

immunohistochemistry, it was found that the ki67 protein content in the lung of urethane-induced lung cancer model mice was significantly increased. The content of cleaved caspase-3 in the shikonin group, the aconitine group and the notoginsenoside R1 group was reduced compared with the model group. The ki67 protein content in the compound group was significantly lower, which was close to the normal value, as shown in Fig. 5A, B. The content of cleaved caspase-3 protein in lungs of urethane-induced lung cancer mice was significantly increased. The content of cleaved caspase-3 protein in shikonin group, aconitine group and notoginsenoside R1 group was increased compared with the model group. The cleaved caspase-3 protein content of the compound group was even higher than the normal value, which was close to the normal value, as shown in Fig. 5C and D.

3.4. Protein expression results in lung tissue

As shown in Fig. 6, the expression of connexin43 and E-cadherin protein in the lungs of the model group mice was very low, indicating that the proliferation and differentiation ability of the cells was decreased, and the adhesion ability between cells was decreased, as shown in Fig. 6A, B, and C. And the expression of tumor stem cell

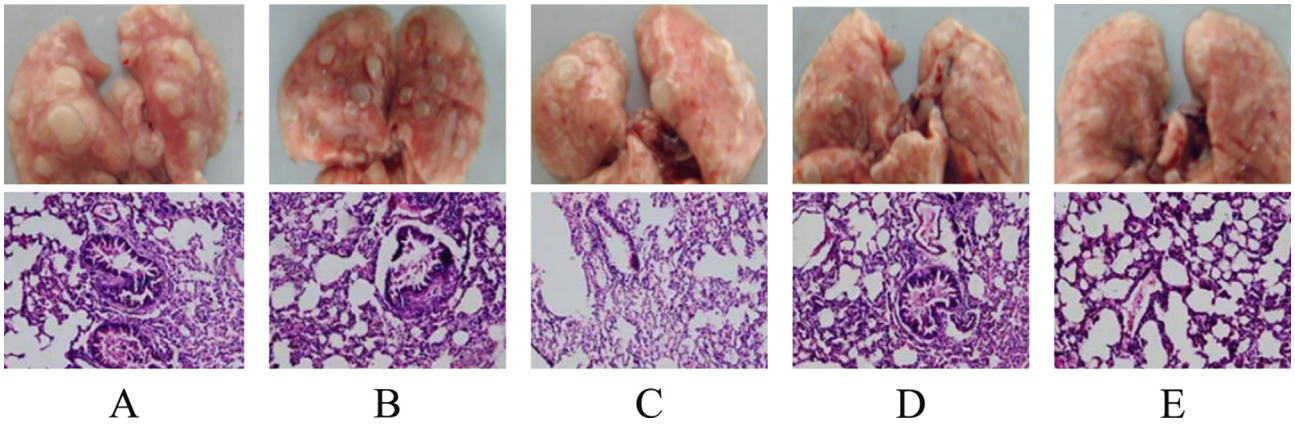

Fig. 4. Picture of lung tissue and HE staining of mice in each group. (A: lung tissue and HE staining of model group mice B: lung tissue and HE staining of shikonin group mice C: lungs tissue and HE staining of aconitine group mouse D: lung tissue and HE staining of mice in the Panax notoginseng R1 group E: lung tissue and HE staining of the mice in the compound group).

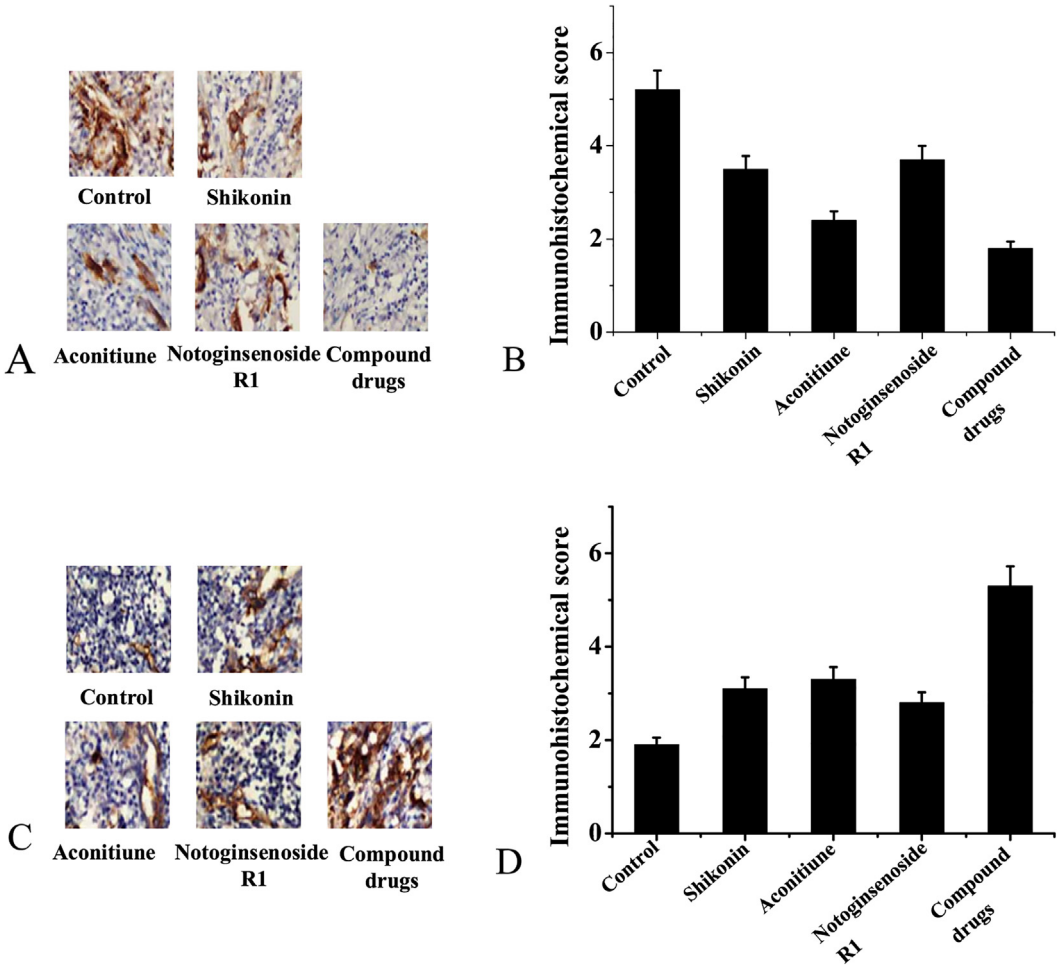

Fig. 5. Immunohistochemical results. (A: Immunohistochemical expression of ki67 in each group B: Semi-quantitative analysis of immunohistochemical expression of ki67 in each group C: Immunohistochemical expression of Cleaved caspase-3 in each group D: Semi-quantitative analysis of immunohistochemical expression of Cleaved caspase-3 in each group).

markers Oct4 and Nanog in the lungs of the model group mice increased. After drug treatment, the expression of connexin43 and E-cadherin protein in the lungs of mice in each treatment group increased, and the expression levels of Oct4 and Nanog decreased. As shown in Fig. 6D, E, and F.

3.5. Results of dye trace method

As shown in Fig. 7, the mouse model group of urethane-induced lung cancer had a low intercellular communication, and the three drugs had a recovery function for the intercellular communication

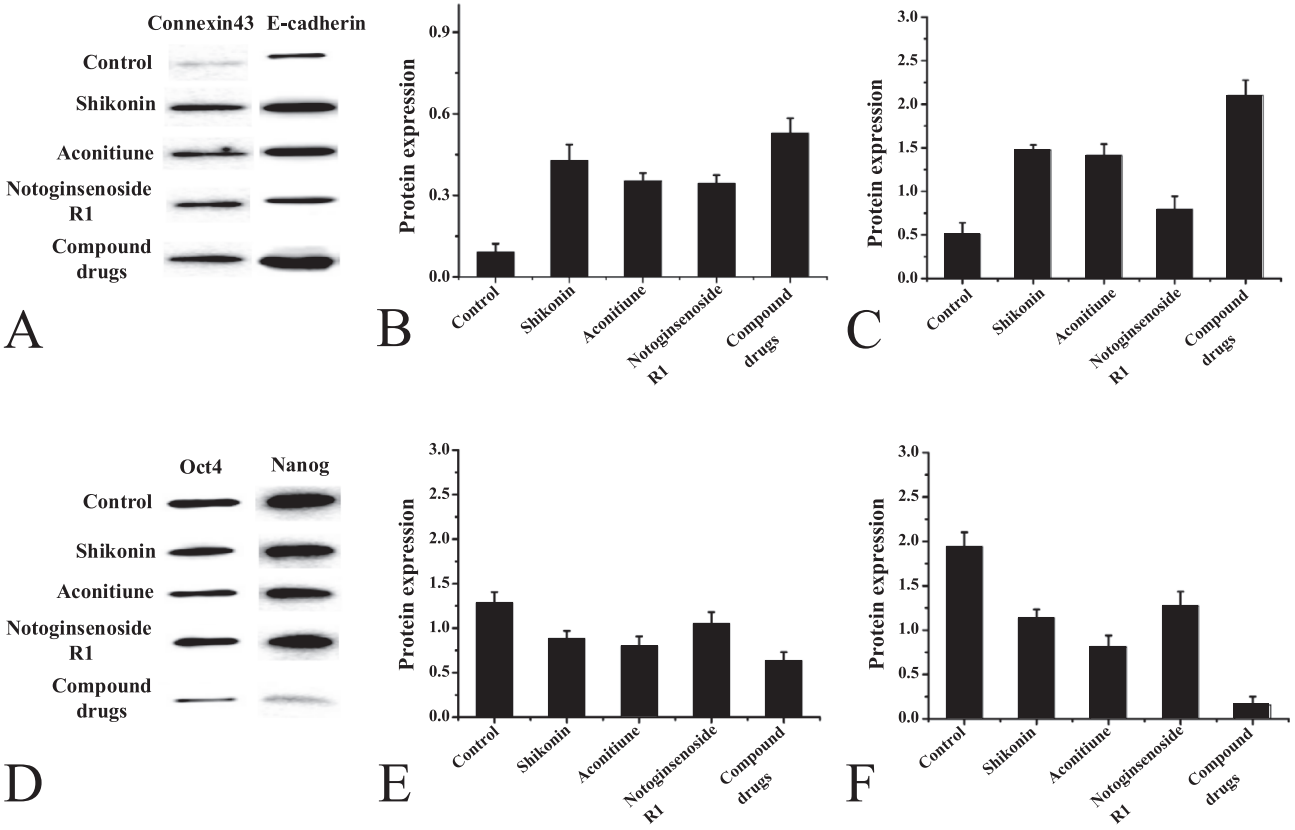

Fig. 6. Protein expression in lung tissue of mice in each group. (A: electrophoretogram of connexin43 and E-cadherin protein expression B: quantitative analysis of connexin43 protein expression C: quantitative analysis of E-cadherin protein expression D: electrophoretogram of Oct4 and Nanog protein expression E: Quantitative analysis of Oct4 protein expression F: Quantitative analysis of Nanog protein expression).

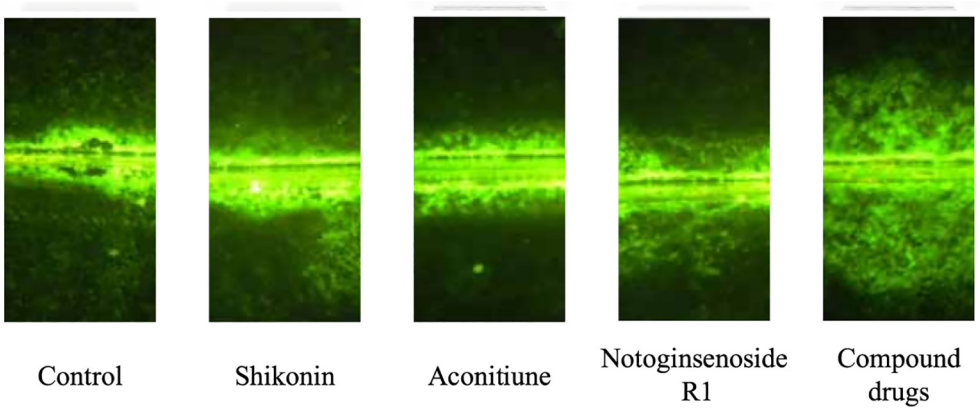

Fig. 7. Effect of three drugs on intercellular communication of urethane-induced cells.

of mice, and the compound group basically restored the intercellular communication of the mice to the normal level.

4. Conclusion

In the mouse model of lung cancer induced by urethane, the anti-cancer effect on mice was studied by using shikonin, aconitine, notoginsenoside R1 and combination of three drugs. The results showed that the body weight fluctuations of the mice in the modeling stage were all first decreased, then stabled and finally recovered. However, the weight of the mice treated by the drug intervention recovered quickly. In the observation of the autonomic activity of mice, the decline of autonomic activity in the model group was extremely obvious, while the autonomic activity of mice using the drug basically returned to normal. After studying the lung tissues of each group of mice, it was found that the permeability of the lung barrier of the model group was significantly increased, and obvious white nodules appeared on the lung tissue, which showed obvious pathological changes. Furthermore, immunohistochemical staining showed that the expression of proteins associated with cell proliferation and differentiation was reduced, and the expression of related proteins in cancer stem cells increased. After the drug intervention in the model mice, the previous conditions were improved to varying degrees, and the

indicators of the mice with intervention of combining three drugs were close to normal values. The connection communication of mouse cells was studied by dye trace method, and it was found that the cell connection communication level of the model group mice was very low, and the drug had an enhanced effect on cell connection communication. Through statistics data, it was found that in the mice model of lung cancer induced by urethane, the control group had a lung cancer incidence rate of 100%, the incidence of lung cancer in the shikonin group was 75%, the incidence of lung cancer in the aconitine group was 50%, and the incidence of lung cancer in the ginsenoside R1 group was 66.7%, while the incidence of lung cancer in the compound group was only 8.3%. This study demonstrated that the combination of shikonin, aconitine and notoginsenoside R1 had a good anti-cancer effect, which provided a theoretical basis for clinical research.

References

Zhang, X., Liu, Y., Peng, X., et al., 2018. Influence of the vaccinating density of A549 cells on tumorigenesis and distant organ metastasis in a lung cancer mice model. Cellular Mol. Biol. (Noisy-le-Grand, France) 64, 53–57.

Szczepny, A., Rogers, S., Wsn, J., et al., 2017. The role of canonical and non-canonical hedgehog signaling in tumor progression in a mouse model of small cell lung cancer. Oncogene 36 (39), 5544–5550.

Yan, X., Wang, L., Zhang, R., et al., 2017. Overcoming resistance to anti-PD immunotherapy in a syngeneic mouse lung cancer model using locoregional virotherapy. Oncoimmunology 7, (1) e1376156.

Luo, Bin, Que, Zu-jun, Zhou, Zhi-yi, et al., 2018. Feiji Recipe inhibits the growth of lung cancer by modulating T-cell immunity through indoleamine-2,3-dioxygenase pathway in an orthotopic implantation model. J. Integr. Med. 19 (4), 1340.

Ramirezalcantara, V., Bing, Z., Xi, C., et al., 2017. Abstract 1140: Characterization of a novel PDE10 inhibitor in lung tumor cells and an orthotopic mouse model of lung cancer. Cancer Res. 77 (13 Supplement). 1140 1140.

Meraz, I.M., Majidi, M., Shao, R.P., et al., 2017. Abstract 621: Tumor suppressor TUSC2 immunogene therapy is synergistic with anti-PD1 in lung cancer syngeneic mouse models. Cancer Res. 77 (13 Supplement). 621–621.

Ehlerding, E.B., England, C.G., Majewski, R.L., et al., 2017. ImmunoPET imaging of CTLA-4 expression in mouse models of non-small cell lung cancer. Mol. Pharm. 14 (5), 1782–1789.

Harshbarger, W., Gondi, S., Ficarro, S.B., et al., 2017. Structural and biochemical analyses reveal the mechanism of glutathione S-transferase Pi 1 inhibition by the anti-cancer compound piperlongumine. J. Biolog. Chem. 292 (1), 112.

Sato, T., Morita, M., Tanaka, R., et al., 2017. Ex vivo model of non-small cell lung cancer using mouse lung epithelial cells. Oncol. Lett. 14 (6), 6863–6868.

Pyo, K.H., Lim, S.M., Kim, H.R., et al., 2017. Establishment of a conditional transgenic mouse model recapitulating EML4-ALK-positive human non-small cell lung cancer. J. Thoracic Oncol. Off. Publ. Int. Assoc. Study Lung Cancer 12 (3), 491–500.

Lakshmanan, I., Rachagani, S., Ponnusamy, M., et al., 2017. Abstract 2825: Gene expression profile in genetically engineered mouse model of lung cancer correlates with that in human lung adenocarcinoma. Cancer Res. 77 (13 Supplement). 2825–2825.

Perepelyuk, M., Shoyele, O., Birbe, R., et al., 2017. siRNA-encapsulated hybrid nanoparticles target mutant K-rasand inhibit metastatic tumor burden in a mouse model of lung cancer. Mol. Therapy Nucl. Acids 6 (C), 259–268.

Menter, David G., Kopetz, Scott, Hawk, Ernest, et al., 2017. Platelet "first responders" in wound response, cancer, and metastasis. Cancer Metastasis Rev. 36 (1), 1–15.

Best, Sarah A., De Souza, David P., Kersbergen, Ariena, et al., 2018. Synergy between the KEAP1/NRF2 and PI3K pathways drives non-small-cell lung cancer with an altered immune microenvironment. Cell Metabol. 27 (4), 935.

Li, Hong, Tan, Ling, Zhang, Jia-Wei, et al., 2019. Quercetin is the active component of Yang-Yin-Qing-Fei-Tang to induce apoptosis in non-small cell lung cancer. Am. J. Chinese Med. 47 (4), 879–893.